Polymorphic transformation from body-centered to face-centered cubic vanadium metal during mechanosynthesis of nanostructured vanadium nitride determined by extended x-ray absorption fine structure spectroscopy

Cite as: J. Appl. Phys. **104**, 023519 (2008); https://doi.org/10.1063/1.2958324
Submitted: 10 September 2007 . Accepted: 28 May 2008 . Published Online: 23 July 2008

Víctor López-Flores, Manuel A. Roldán, Concepción Real, Adela Muñoz Páez, and Germán R. Castro

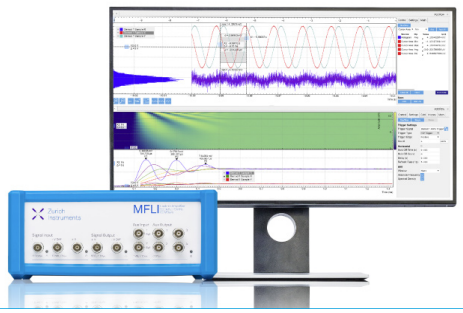

Polymorphic transformation from body-centered to face-centered cubic vanadium metal during mechanosynthesis of nanostructured vanadium nitride determined by extended x-ray absorption fine structure spectroscopy

Víctor López-Flores,[1] Manuel A. Roldán,[1] Concepción Real,[1] Adela Muñoz Páez,[1,a)] and Germán R. Castro[2]
[1]*Institute of Materials Science of Seville, Inorganic Chemistry Department, CSIC, University of Seville, Av. Americo Vespucio, No. 49, 41092 Seville, Spain*
[2]*SpLine CRG at the European Synchrotron Radiation Facility, BP220, F-38043 Grenoble Cedex, France*

(Received 10 September 2007; accepted 28 May 2008; published online 23 July 2008)

The pathway for vanadium nitride (VN) formation obtained by milling treatment has been traced out. At the initial stages of the process, the reactant, vanadium metal, showing body-centered cubic (bcc) structure, becomes highly distorted. Simultaneously, the formation of a small nucleus of the product, VN, takes place. X-ray absorption spectroscopy (XAS) has allowed the quantification of the distortion degree as well as the detection of the VN nucleus in the early stages of their formation, while other standard structural characterization techniques are unable to detect such phenomena. For increasing milling times, apart from the expected increase in the size of the VN nucleus, a polymorphic transformation from bcc to fcc vanadium metal has been recorded. This phase might play a key role in the overall synthesis process and could be a reaction intermediate in other solid state processes involving V metal. The sensitivity of XAS to noncrystalline domains and to highly distorted environments, as well as the use of high resolution x-ray diffraction, has provided the relevant information to understand the whole reaction process. © *2008 American Institute of Physics*. [DOI: 10.1063/1.2958324]

I. INTRODUCTION

Transition metal nitrides have attracted much attention in the past few years due to their special properties.[1] In particular, the cubic vanadium nitride (δ-VN) has extreme hardness, high thermal and electrical conductivity, and corrosion resistance.[2,3] These properties make it a suitable component for many uses, such as cutting tools, structural materials, magnetic and electric components, and superconducting devices, as VN is a superconductor with a transition temperature ranging from 2 to 9 K.[3–5] Conventionally, it is prepared by direct nitridation of pure metal or by carbothermal reduction in other compounds, both processes under nitrogen or ammonia atmosphere above 1000 °C.[6,7] Recently, several other methods have been employed to synthesize VN; for instance, reactive magnetron sputtering deposition, ammonolysis of precursor compounds of the metal, thermal reduction-nitridation in an autoclave, solid state metathesis, or self-propagating high temperature synthesis, to name but a few.[8–11] On the other hand, mechanical alloying via ball milling is considered as a method to synthesize nanoparticulated materials at room temperature such as amorphous phases, supersaturated solid solutions, metastable phases, intermetallic compounds, composites, and ceramic materials.[12–15] Thus, several metal nitrides have been obtained by ball milling of elemental powders in nitrogen or in dry ammonia atmospheres.[16–18] VN has been obtained from mechanical treatment by Calka and Williams[19] using a planar type ball mill under nitrogen atmosphere with a milling time of 60 h. To improve synthesis methods, a deep knowledge of the reaction mechanism is needed. Unfortunately, samples submitted to mechanical treatments show a high degree of disorder, so it is difficult to get detailed structural information about the species involved in the process.

X-ray absorption spectroscopies (XASs) both from the high energy region [extended x-ray absorption fine structure (EXAFS)] and the low energy region [x-ray absorption near edge structure (XANES)] provide chemically specific short range structural information. They are well suited to investigate the local atomic environment around medium to heavy elements,[20] since they do not require long range structural order. Moreover, the method can equally be applied to samples in crystalline or amorphous form. For these reasons, XAS is a unique tool to trace structural changes along the reaction progress.

In this work we present the results of the synthesis of VN by ball milling of metallic vanadium under nitrogen atmosphere at a pressure of 11 bars, with an exceptionally short milling time of 8 h. The characterization of the final product as well as that of the compounds at intermediate states has been carried out using high resolution x-ray diffraction (HR-XRD) to analyze the crystalline phases. Moreover, to track the existence and evolution of phases lacking long range order, XAS has been used. With the aid of this technique it was found that ball milling treatment induced a high degree of amorphization, and that a significant amount of the stoichiometric VN, δ-VN, was formed after very short

a)Electronic mail: adela@us.es.

milling times. Moreover, an intermediate vanadium metal phase with face-centered structure was found during the synthesis process.

II. EXPERIMENTAL

Vanadium powder with a purity of 99.5% (Aldrich) was milled under pressure at 11 bars of high purity nitrogen gas (H_2O and $O_2 < 3$ ppm) using a modified planetary ball mill (Fritsch, model Pulverisette 7). A steel vial of 45 cm^3 with six steel balls was used. The diameter and weight of the balls were 15 mm and 13.85 g, respectively. 5 g of V powder was introduced in the vial, so the powder-to-ball mass ratio was 1:16. In the vial, previously purged with nitrogen, the desired nitrogen pressure was selected before starting the milling process. The vial and the gas cylinder were connected through a rotary valve and a flexible polyamide tube, which allows working pressures of up to 27 bars.[21] The rotary valve can operate up to 25 000 rpm under pressures ranging from vacuum to 70 bars. In this way, the vial was permanently connected to the gas cylinder that supplies the gas at the desired pressure over the whole process. A spinning rate of 700 rpm for both the rotation of the supporting disk and the superimposed rotation in the opposite direction of the vial was used.

X-ray powder diffraction patterns were collected both in a laboratory diffractometer and at a synchrotron radiation source. The first was recorded with a Siemens D501 instrument equipped with a scintillation counter using Cu $K\alpha$ radiation and a primary graphite monochromator; the scanning rate of the goniometer was 0.4 °min^{-1}. The second was recorded at branch A of BM25 (SpLine CRG) beamline at the European Synchrotron Radiation Facility (ESRF) at Grenoble, France, operating at 6 GeV, with a maximum stored current of 200 mA. The incident radiation of 18.8 keV was obtained with a Si (311) double crystal monochromator.[22] The scanning rate of the goniometer was 0.1 °min^{-1}. The lattice parameter refinement of the crystalline domains of the samples was calculated from the whole set of peaks of the XRD diagram using the LAPODS computer program[23] and assuming a bcc structure for V metal and the fcc rocksalt type structure for δ-VN.

Thermogravimetric (TG) diagrams were recorded for the vanadium samples submitted to increasing times of milling treatment, at a heating rate of 5 °C/min from room temperature up to 1400 °C, using a nitrogen flow of 100 cm^3/min, at a pressure of 1 bar. The conversion of V into VN during the milling process was calculated from the mass gains, assuming that the final product was the stoichiometric nitride δ-VN. The validity of this indirect method was checked by recording the total mass gain during the nitriding process of a pure V unmilled sample. The iron contamination coming from the mill vial was calculated by Fe^{2+} permanganimetry. This iron was eliminated by HCl leaching.

The oscillatory part of an x-ray absorption spectrum can be described as the sum extended over j neighboring coordination shells of atoms around the absorbing atom.[20]

$$\chi(k) = \sum_j \frac{N_j}{kR_j^2} S_0^2 F_j(k) e^{-2k^2\sigma_j^2} e^{-2R_j/\lambda(k)} \sin[2kR_j + \varphi_j(k)], \quad (1)$$

where k is the photoelectron wave vector and N_j is the coordination number of the atoms in shell j at a coordination distance R_j. S_0^2 is the amplitude reduction factor due to many body effects. $F_j(k)$ is the backscattering amplitude function of each kind of neighboring atom, $\varphi_j(k)$ is the total phase shift of the photoelectron, λ is the photoelectron mean free path, and σ_j^2 is the Debye–Waller factor, accounting for static and dynamic disorder, for shell j. Since $F_j(k)$ and $\varphi_j(k)$ are functions characteristic of each pair of absorbing and backscattering elements, the technique is element sensitive. S_0^2 and λ can be estimated, while $F_j(k)$ and $\varphi_j(k)$ can be accurately calculated for each pair of atoms, so that the fit of the experimental signal yields the structural parameters R_j, N_j, and σ_j^2. Since this spectroscopy implies scattering phenomena, the obtained parameters are similar to those obtained from x-ray diffraction, although they show a higher degree of indetermination. On the other hand, this spectroscopic technique provides average information about all the regions around the selected element, both crystalline and amorphous.

XAS spectra at the V-K edge (E=5465 eV) of the samples submitted to 0.5, 1.5, and 8 h milling times were recorded at the synchrotron radiation source ESRF in Grenoble, France, at station BM29. The ring energy was 6 GeV and the maximum stored current was 200 mA. A double crystal Si (311) monochromator was used. Higher harmonic rejection was carried out by detuning both crystals to 50% of the intensity of the first harmonic. Measurements were carried out at room temperature in transmission detection mode, using 45 cm ionization chambers as detectors, filled with the appropriate gas mixtures. The amount of sample used was that calculated to attain the optimum absorption μx=2.5. Since the required amount of sample was rather small (a few milligrams), they were mixed with BN to reach the minimum value, around 100 mg, to prepare a self-supported wafer.

Standard methods were used to perform background subtraction and normalization of the EXAFS spectra, as explained elsewhere.[24] Thus, the EXAFS functions $\chi(k)$ were obtained from the x-ray absorption spectra by subtracting a Victoreen curve followed by a cubic spline background removal using the program AUTOBK,[25] and were normalized to the height of the measured absorption edge. E_0 was defined as the energy where the absorption coefficient is one-half of the height of the atomic absorption jump. The EXAFS spectra thus obtained were analyzed by the nonlinear least-squares fit approach of the FEFFIT 2.984 program,[26] using the phase shift $\varphi_j(k)$, and backscattering amplitude functions $F_j(k)$, calculated with the FEFF 6.02 code.[27] To fit the spectra, the single scattering (SS) paths corresponding to each coordination shell were used. Besides, the multiple scattering (MS) paths involving colinear atoms were taken into account because these have high amplitude and represent a significant contribution to the EXAFS signal.[28] In the systems studied here, one of such paths is the one including the first and fourth coordination shells of the δ-VN nitride (with a rock-

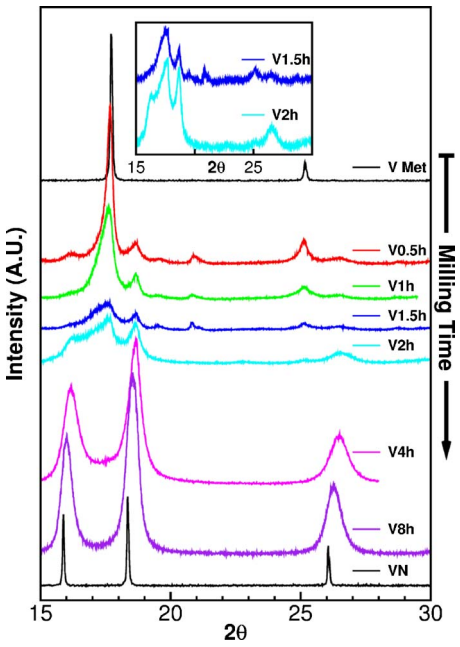

FIG. 1. (Color online) Synchrotron radiation HR-XRD diagrams at 18.8 keV for the samples one year after being submitted to milling treatments at increasing times, including V-bcc metal and δ-VN references.

salt structure). A curved wave amplitude filter was used, according to which only paths with an amplitude equal to or higher than 15% of the most intense path, obtained by integrating through the fitting range, were taken into account. Only those paths whose maximum effective distance is equal to or smaller than 5.5 Å were considered.

Taking into account all the species involved in the reaction process, i.e., the reactant vanadium metal and the products, VNs, model structures for V metal and nitrides, δ-VN, and β-V_2N, the structures were taken into account to fit the data. To reduce the number of free parameters, the Debye–Waller factors required for the MS paths were derived from the corresponding SS paths applying the relationships of the independent vibration model.[29] This approach has proven to be accurate for similar analysis on the $[Cr(H_2O)_6]^{3+}$ and $[Rh(H_2O)_6]^{3+}$ aqua ions as deduced from combined EXAFS and molecular dynamics calculations.[30] The amplitude reduction factor S_0^2 was set to 0.81 for all the environments. This is a value within the range of values reported in literature,[24,31] which rarely varies for the same element at different chemical environments.

III. RESULTS

Figure 1 shows the x-ray diffraction patterns of the vanadium samples milled for increasing time length. The diffractograms of the unmilled V metal sample and of a δ-VN sample obtained by carbothermal reduction in V_2O_5 in N_2 atmosphere have been included as well for comparison. This figure shows a gradual evolution from the initial reactant V metal with a bcc structure to the final product cubic δ-VN with a rocksalt structure.[32] After 0.5 h of milling time, the peak heights of V metal decrease drastically, indicating a disruption of the metallic environment caused by the milling treatment. At the same time, wide peaks appear around the δ-VN peak positions.[32] In the sample submitted to 1 h of milling treatment, the most intense peak of V metal remains at 17.6°, but its intensity decreases further and its width increases, while the other V-metal peak at 25.1° is barely seen. The maxima at the δ-VN positions maintain their intensity. In the 1.5 h sample, this tendency progresses, so the V metal main peak almost disappears, while the δ-VN ones remain almost the same. After 2 h of milling treatment, the two wide peaks corresponding to δ-VN, at 16.2° and 18.7°, emerge and increase their intensity over the remains of the main V metal peak. The height of these peaks increases and its width decreases for longer milling times, so that after 8 h of milling treatment they have its maximum height. Furthermore, the smaller diffraction peak of δ-VN, at 26.6°, has appeared. As shown in Table I, increasing times of milling treatment induce an increase in the lattice parameter of V metal and of δ-VN. In the 1.5 h sample, the lattice parameter for V-bcc is 3.05 Å (the starting value was 3.03 Å), while that of δ-VN is 4.11 Å (the starting value was 4.08 Å). No evidence of the βV_2N crystalline phase was found in any of the samples.[32] In addition to the peaks corresponding to both V and δ-VN species, a small maximum appeared at around 21° in the samples submitted to 0.5, 1.0, and 1.5 h milling times. These peaks, completely missing in the laboratory diffractograms, can be attributed to the existence of VO_x species.[33] It has to be taken into account that the HR-XRD was recorded one year after they were prepared, so the appearance of the additional peaks can be related to the aging process. The intermediate samples are the ones that should present the highest concentration of defects, so that surface oxidation reactions yielding VO_x species can progress in an easier way.

TABLE I. V/δ-VN ratio obtained from thermogravimetry, crystalline lattice parameter from XRD, and Fe contamination from permanganimetry.

Milling time (h)	Composition (%) V	Composition (%) δ-VN	Lattice parameter (Å) V	Lattice parameter (Å) δ-VN	Fe (wt. %)
0	100	0	3.03	-	0
0.5	90	10	3.03	-	5.2
1	90	10	3.03	-	7.2
1.5	84	16	3.05	-	6.1
2	61	39	-	-	6.8
4	35	65	-	4.08	6.5
8	10	90	-	4.11	8.9

Figure 2 shows the TG diagrams of the milled samples obtained under nitrogen flow, as well as that of a metallic vanadium sample, included for comparison. The V/VN ratio for each sample was calculated from the mass gain, assuming that the only nitride phase formed is the stoichiometric δ-VN. These ratios have been included in Table I.

The chemical analysis of the total iron content suggested that the contamination by this metal took place during the milling treatment, since the total amount increased with time, reaching a maximum value of 8.9% after 8 h of milling treatment. It was completely removed rinsing the samples with diluted hydrochloric acid. Iron contamination was not observed in the XRD patterns. This can be due either to the fact that iron contamination does not form crystalline domains or because the position of the Fe-bcc diffraction maxima is

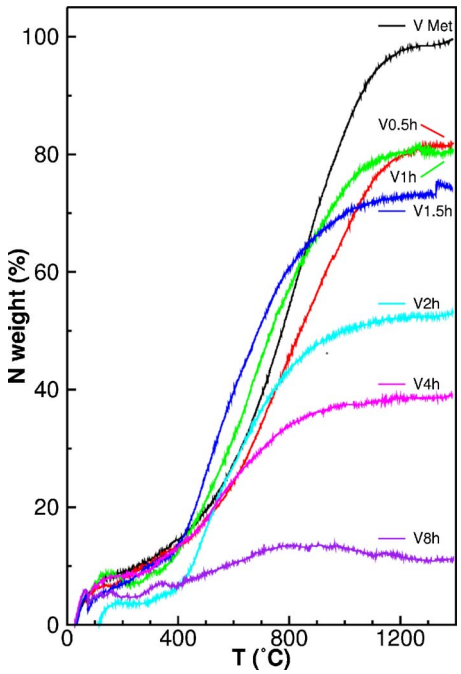

FIG. 2. (Color online) TG diagrams for the samples submitted to milling treatments at increasing times.

close to that of V and δ-VN diffraction peaks and, since these peaks are rather wide, they can hide Fe ones.

The normalized XANES spectra of the V-*K* absorption edge appearing at 5465 eV for the three the samples have been included in Fig. 3. The V-*K* edge is rather sensitive to coordination environment and oxidation state. For this reason, its overall shape has been used as a fingerprint by comparing it with that of other crystalline compounds of known structure.[34] The XANES spectra of sample V0.5h resemble

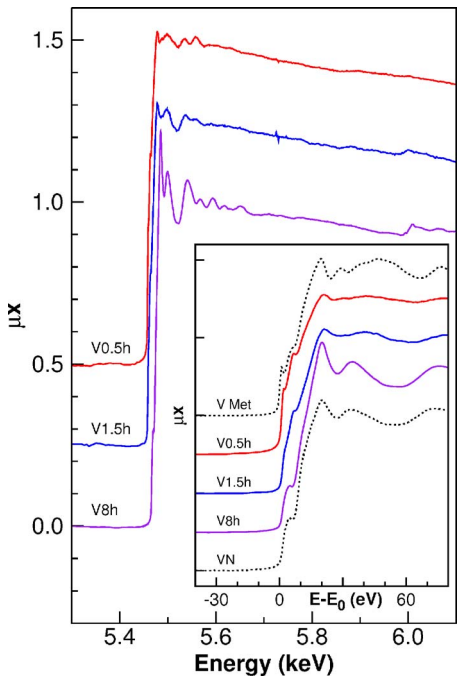

FIG. 3. (Color online) XAS spectra for V0.5h, V1.5h, and V8h samples and the insight of the XANES region, including V metal and δ-VN spectra for comparison.

that of the vanadium metal, while that of sample V8h is similar to the spectrum of the VN compound, as can be deduced from the comparison with the corresponding spectra included in the inset, taken from Ref. 35. In the V1.5h sample spectrum there seems to be an intermediate situation between the two previous XANES spectra: While maintaining the higher energy shoulder of the V0.5h spectrum, there is a hint of another shoulder at lower energies similar to that appearing in the V8h spectrum. Besides, the absorption edge energy is between the previous ones, as expected for a system with an intermediate oxidation state.

The intensity of the EXAFS oscillations of the three spectra is rather low, particularly those of V0.5h and V1.5h samples. This low intensity indicates that these samples should show a high degree of amorphization. In addition to the XAS spectra of the V-*K* edge, the figure shows a small step at 6000 eV approximately, which is the position of the x-ray absorption Cr-*K* edge. Its origin is probably due to a contamination of chromium from the mill used, which is made of stainless steel with added chromium. This assumption is consistent with the fact that the step is higher for longer milling times, which means a higher chromium concentration, in a behavior parallel to iron contamination detected by permanganimetry. Chromium content in the steel from the mill is estimated to be around 9%, so a similar ratio should be expected for the contaminations of Fe and Cr. According to this assumption, the maximum value expected for chromium content is around 0.8%.

The starting models used to fit the EXAFS spectra were those corresponding to the crystalline structures of the species detected by XRD, V-bcc, and δ-VN. In addition, a V-fcc structure, similar to those described by Manna and coworkers for Nb,[36] Ti,[37] and Zr,[38] was taken into account. A single free parameter a, which stands for the lattice parameter, was used to allow the coherent variation of the coordination distances for all the coordination shells. The respective coordination numbers were fixed to those of the perfect crystal structures in each case. The Debye–Waller (σ^2) factors were allowed to vary independently for each coordination shell. Due to the highly distorted nature of these milled samples, the main reason for the spread of coordination distances around the average value is the static disorder caused by the deformation from the ideal structure. This high disorder is a consequence of the high number of defects.

Furthermore, the reduction in the particle size due to the milling process will increase the surface/bulk atom ratio. A similar effect can be found in the boundary between two different phases inside the same particle, e.g., the reactant and products, so there is a high concentration of defects at this interface, as it happens in the external surface of a particle. Since surface atoms have a lower coordination number and XAS gives average information of all the possible absorbing atoms regardless its position, the existence of such an interface will decrease the mean coordination numbers for all the shells. This high content of structural defects and, as a consequence, of vacancies in these samples required the use of an additional variable to simulate the proportional reduction in the coordination numbers for all the shells. Thus, a variable D was set as a linear scale factor affecting the co-

TABLE II. Fitting parameters for sample V0.5h obtained from EXAFS analysis. N are the coordination numbers (fixed to crystalline values), R are the coordination distances (calculated from the lattice parameter), and σ^2 are the Debye–Waller factors (independent variable for each shell).

	V-bcc					δ-VN				
Lattice parameter	3.02 Å					4.02 Å				
Shell	1 (V)	2 (V)	3 (V)	4 (V)	5 (V)	1 (N)	2 (V)	3 (N)	4 (V)	5 (N)
N	8	6	12	24	8	6	12	8	6	24
R (Å)	2.62	3.02	4.27	5.01	5.23	2.01	2.84	3.48	4.02	4.49
σ^2 (Å^2)	0.006	0.008	0.012	0.013	0.014	0.007	0.008	0.010	0.017	0.019

ordination numbers at all the scattering paths taken into account in the fit of the EXAFS spectra. Although this is rather unusual, it was previously observed in a lutetium intercalated layered silicate submitted to hydrothermal treatment[39] and during the solid state reaction process of several oxides.[40] This variable would range from 0 (for a sample with atoms lacking any order even in the first coordination shell) to 1 (if the sample was a perfect crystal). Moreover, since it could be related to the surface/bulk atom ratio, the variable D can give a hint about the size of the particles. Some attempts to establish quantitative relationships between coordination number reduction and the particle size can be found in literature.[41,42] Unfortunately, factors such as the shape of the particles and concentration of defects among others make this approach highly inaccurate. Thus, the physical meaning of the D variable should remain as the qualitative relationship described above.

V0.5h sample: Since according to the XRD results, shown in Fig. 1, the major component of this sample was the reactant, a V metal with a bcc structure, the spectrum was initially fitted with the first five coordination shells of the V-bcc metal. However, the fit was not good enough, so a different approach was made. The x-ray diffractogram recorded at the synchrotron radiation source included in Fig. 1 also showed some hints of δ-VN. Thus, the first five coordination shells of this structure were added. These shells are those which interfere with V-bcc metal shells. A mixture of both structures was found in a ferritic steel with V added, submitted to nitriding treatments.[43] As described above, the variables were the lattice parameters a for both structures, the Debye–Waller factor for each shell, and the coordination number reduction factor D for both structures. Two values of energy shift E_0 were used, one for each environment, being 3 eV higher for δ-VN paths. This value was chosen due to the energy shift in the absorption edge caused by the formal oxidation from (0) in the V metal to (III) in VN. The ratio of V-bcc/δ-VN was fixed to the values deduced from TG, equal to 90/10 in this sample. This made a total of 15 free parameters: a(V), a(δ-VN), 5+5 Debye-Waller factors, D(V), D(δ-VN), and E_0(V). This number of variables is well below the upper limit given by the derivation of the Nyquist theorem for XAFS spectra:[44]

$$N_I = \frac{2\Delta k \Delta R}{\pi} + 2, \tag{2}$$

where N_I is the number of independent points and Δk and ΔR are the ranges of the spectrum in k space and R space, respectively. In this case, N_I is around 20. Taking into account both environments, the fit improved significantly. The results of the fit are shown in Table II. The experimental and best fit spectra in the k space are shown in Fig. 4, while those in the R space are shown in Fig. 5.

V1.5h sample: Although this sample did not show any well defined crystalline structure, it showed wide peaks in the x-ray diffractogram where the maxima for V-bcc and δ-VN should appear. The EXAFS spectrum was initially fitted with a pure δ-VN model up to the fifth coordination shell. However, the fit was not good enough. As the starting reagent was V-bcc metal powder, there could be some remaining V metal. Thus, metallic V-bcc was included in the simulation, varying the Debye–Waller factors and the lattice parameter independently, as explained for the previous sample. Again, the V-bcc/δ-VN ratio was set to the values given by TG, 84/16, while the variable D was independent for each environment. Energy shifts E_0 were varied as in the previous sample. The total number of free parameters was also 15 and fit quality was rather good. The results appear in Table III, while the experimental and best fit spectra in k and R spaces are shown in Figs. 4 and 5, respectively.

V8h sample: Taking into account the XRD results, the EXAFS spectrum was initially fitted with a pure δ-VN model up to the fourth coordination shell. The variables used were D, the Debye–Waller factors, and the lattice parameter, as described above. Again, the fit did not yield a good repro-

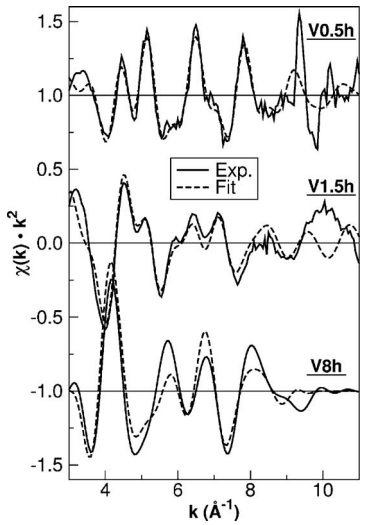

FIG. 4. Experimental and best fit k^2-weighted EXAFS spectra for V0.5h, V1.5h, and V8h samples in k space.

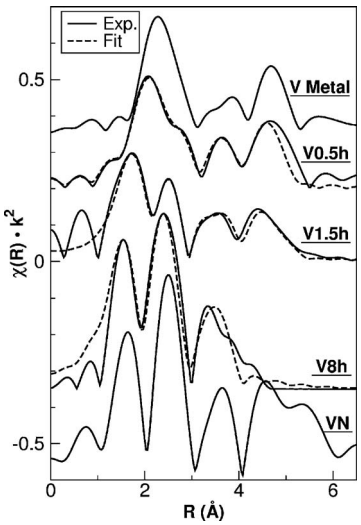

FIG. 5. Experimental and best fit k^2-weighted EXAFS spectra for V0.5h, V1.5h, and V8h samples, including V metal (scaled to 15%) and δ-VN (scaled to 80%) spectra for comparison, in R space (magnitude of the Fourier transform).

duction of the signal with this model. The shape and low intensity of the second peak of the Fourier transform pointed to the fact that there could be two shells interfering destructively at that distance. Besides, since the sample was prepared from V metal powder, there could be some remaining V metal in the sample, as in the previous case. Thus, the V-bcc environment was included in the fit in a way similar to that described above. However, the model failed again and, for this reason, the existence of a different structure was proposed.

It has been shown that the milling treatment can induce phase transformations.[17] More specifically, Manna and coworkers confirmed this effect for Nb,[36] Ti,[37] and Zr metal phases.[38] For these reasons, the possibility of having a polymorphic transformation in the V metal induced by the milling treatment was considered. Thus, the spectrum was fitted with a mixture of δ-VN and metallic V-fcc in the same fashion as described for the previous samples, using the first two shells of the latter structure. In this case, the number of free parameters was 11. As seen in Figs. 4 and 5, including both the experimental and best fit spectra in k and R spaces, respectively, the results of the fit within this approach were rather good. The fit parameters are included in Table IV. To show only the relevant shells, the spectrum was Fourier filtered so that the signal above 4 Å was removed.

The values of D parameter for the three samples and the structures used in the models are summarized in Table V. Sample V0.5h, with 90% V-bcc according to TG, shows the lowest D value for V-bcc (0.2). After 8 h of milling treatment the novel V-fcc phase is detected.

TABLE IV. Fitting parameters for sample V8h obtained from EXAFS analysis. N are the coordination numbers (fixed to crystalline values), R are the coordination distances (calculated from the lattice parameter) and σ^2 are the Debye–Waller factors (independent variable for each shell).

	V-fcc		δ-VN			
Lattice parameter	3.80 Å		4.12 Å			
Shells	1 (V)	2 (V)	1 (N)	2 (V)	3 (N)	4 (V)
N	12	6	6	12	8	6
R (Å)	2.69	3.80	2.06	2.91	3.57	4.12
σ^2 (Å^2)	0.005	0.006	0.007	0.014	0.015	0.019

IV. DISCUSSION

The whole set of results from TG, XRD, and EXAFS can be understood by assuming that pure metallic V submitted to a milling process under N_2 atmosphere follows the reaction processes described below. Note that the information obtained from XRD and EXAFS techniques is complementary, since the first informs about crystalline domains and the second about *both* crystalline and amorphous domains.

The initial 0.5 h of milling treatment induces a significant particle size reduction as well as a distortion of the sample structures, as shown by the widening of the XRD peaks, the reduction in parameter D, and the high Debye–Waller factors in the EXAFS spectrum. A similar effect was already observed by other authors after submitting the samples to milling treatments.[17,19] This can be due to the increase in the number of defects, thus yielding a highly disordered structure with high Debye–Waller factors. Moreover, there is a reduction in the particle size, thus increasing the surface/bulk atom ratio. Since surface atoms have a lower coordination number for all the coordination spheres,[42] D decreases. In this sample, VN formation is at its first stage. It should be noted that the D parameter of the V-bcc environment is lower than that of the δ-VN environment. This reflects the fact that VN is mechanically more resistant than V, so the milling process creates defects more effectively in the structure of the latter.

TABLE III. Fitting parameters for sample V1.5h obtained from EXAFS analysis. N are the coordination numbers (fixed to crystalline values), R are the coordination distances (calculated from the lattice parameter), and σ^2 are the Debye–Waller factors (independent variable for each shell).

	V-bcc					δ-VN				
Lattice parameter	3.06 Å					4.04 Å				
Shell	1 (V)	2 (V)	3 (V)	4 (V)	5 (V)	1 (N)	2 (V)	3 (N)	4 (V)	5 (N)
N	8	6	12	24	8	6	12	8	6	24
R (Å)	2.65	3.06	4.32	5.07	5.30	2.02	2.86	3.50	4.04	4.52
σ^2 (Å^2)	0.014	0.021	0.027	0.028	0.033	0.004	0.006	0.015	0.016	0.018

TABLE V. Coordination number reduction factors (D) for samples V0.5h, V1.5h, and V8h obtained from the EXAFS analysis. The percentage of V and δVN as obtained from TG measurements have been included as well.

	D (TG, %)		
Milling time (h)	V-bcc	V-fcc	δ-VN
0.5	0.20(90)	-	0.70 (10)
1.5	0.32(84)	-	0.90 (16)
8	-	0.25 (10)	0.44 (90)

After 1.5 h of milling time, a further distortion takes place, with additional VN formation. Since D values remain similar to those of the previous sample, particle size and the amount of defects have not changed substantially. On the other hand, compared to the previous sample, the Debye–Waller factors increased for V metal while remained similar for δ-VN. This points to the above mentioned fact that the V metal structure is far weaker than the VN one. As deduced from XRD data, probing crystalline domains, and EXAFS, probing both crystalline and amorphous regions, the V-bcc lattice parameter has increased slightly. This is caused by the disruption caused by the milling process and by the introduction of some N atoms in the structure, which expand the lattice in a way similar to that observed in the formation of solid solutions of C or N within several metals.[45] On the other hand, the lattice parameter of the δ-VN environment also increases, but in this case it moves toward the crystalline value (4.14 Å). As the reaction affects a higher proportion of the sample, as deduced from the TG data, the δ-VN structure gets more similar to the crystalline one, concerning coordination distances. Nevertheless, crystalline domains have not appeared yet, so the structural information cannot be obtained from XRD but from the analysis of the EXAFS data.

After 8 h of milling treatment, most of the deformed metal V-bcc has reacted with the nitrogen gas to form the δ-VN phase with a rocksalt structure in which vanadium atoms show a fcc structure. Together with this reaction, the original bcc structure of the V metal seems to undergo a polymorphic transition to a fcc structure, as shown by the results of the EXAFS analysis for sample V8h. This transition might be caused by the high amount of defects plus the high local temperatures induced by the milling process, as it has been described by Manna and co-workers for Nb, Ti, and Zr.[36–39] Furthermore, the first incorporation of N atoms in the V-bcc structure enlarges and ultimately changes the structure as an intermediate state to accommodate further N atoms in it. Finally, the δ-VN structure acts as a driving force to rearrange the structure of neighbor V atoms that do not have N inside their structure yet. The lattice parameter of the δ-VN environment comes even closer to the theoretical value. The D parameter for the δ-VN environment decreases, which is probably caused by the intensive milling this sample has undergone. On the other hand, the Debye–Waller factors decrease for the V-fcc structure, so it seems that the reorganization of the atoms due to the polymorphic transformation reduces the disorder.

The whole set of coordination numbers and distances used to fit the EXAFS spectrum is tied to the V-fcc structure, so any other structure fulfilling these strict relationships would give a different spectrum. From this fact it can be deduced, with a high degree of confidence, that V-fcc is the structure present in the sample. However, this is only valid for the local environment around vanadium. Nothing can be said about the long range order and, in fact, no crystalline domains can be seen in the XRD diffractograms. There are several reasons that might hamper the detection of the V-fcc phase by XRD even in the diagrams recorded at the synchrotron source: (1) The nuclei are probably so small that they lack long range order; (2) the structure is probably extremely distorted; and (3) the possible diffraction peaks would appear very close to the δ-VN ones, so the latter may be hiding them.

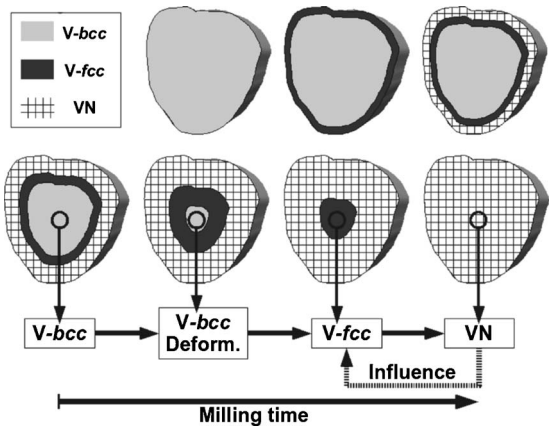

FIG. 6. Model of the transformation process of a particle in the proposed reaction path to obtain δ-VN from V under N_2 atmosphere.

In light of these results, the process occurring in the milled sample could be the following.

(1) The milling treatment distorts significantly the V-metal structure, reducing the particle size, increasing the number of defects, and expanding the V-bcc metal lattice. Thus, the sample becomes highly reactive against N_2, probably enabling the dissociative chemisorption of this gas at its surface, as already proposed by other authors.[19]
(2) The introduction of nitrogen atoms in the V-bcc structure expands the lattice to accommodate them. This, together with the continuous milling process, induces a polymorphic transformation of the V-bcc structure into a V-fcc structure. This transformation, as suggested by Manna and co-workers in Nb, Zr, and Ti, would reduce the surface energy of the metal.[36–38]
(3) This V-fcc structure, yet too tight to accommodate enough N atoms to form the stoichiometic nitride, further expands getting more N atoms in it, becoming more similar to the δ-VN structure.

This is illustrated in Fig. 6. The process does not occur in the whole sample at the same time. The places with a higher local temperature react first, and then influence their surroundings, inducing the change in their structures. In other words, the incipient VN acts like a driving force for the reaction. However, at an intermediate stage, after submitting the sample for 2–4 h of milling treatment, the V-bcc structure

disappears as a whole, as shown in the XRD diagrams and in the EXAFS data, either by transforming into the V-fcc phase or by reacting to form the final product δ-VN.

A model of the reaction process that might occur in each particle is illustrated in Fig. 6. The distortion induced by milling a treatment starts at the surface and progresses toward the core. In parallel, nitrogen is gradually introduced in the particle, forming the δ-VN phase. According to the proposed model, the V-fcc phase should be located at the interface, acting as the reaction intermediate.

ACKNOWLEDGMENTS

We acknowledge the European Synchrotron Radiation Facility (ESRF) for provision of synchrotron radiation facilities and for beam time allocated to carry out the EXAFS measurements at station BM29 under Project No. ME-737. We would like to thank S. Ansell, D. T. Bowron, S. Diaz-Moreno, and S. Ramos for assistance during the measurements. We also acknowledge SpLine CRG (beamline BM25 at the ESRF) for beam time allocated under Project No. 25-01-657 to carry out HR-XRD experiments. We would like to thank A. Gutierrez-León, J. Rubio-Zuazo, and I. da Silva for assistance in the beamline. The Spanish Ministry of Science and Education is acknowledged for financial support under Project Nos. BQU2002-04364-C02-01 and BQU2002-04364-C02-02.

[1] *The Chemistry of Transition Metal Carbides and Nitrides*, edited by S. T. Oyama (Blackie, London, 1996).
[2] A. Glaser, S. Surnev, F. P. Netzer, N. Fateh, G. A. Fontalvo, and C. Mitterer, Surf. Sci. **601**, 1153 (2007).
[3] M. G. Krishna and A. K. Bhattacharya, Int. J. Mod. Phys. B **13**, 833 (1999).
[4] J. Zasadzinski, R. Vaglio, G. Rubino, K. E. Gray, and M. Russo, Phys. Rev. B **32**, 2929 (1985).
[5] N. Sudhakar, R. S. Ningthoujam, K. P. Rajeev, J. Weissmuller, and N. S. Gajbhiye, J. Appl. Phys. **96**, 688 (2004).
[6] L. E. Toth, *Transition Metal Carbides and Nitrides* (Academic, New York, 1971), Vol. 7.
[7] P. K. Tripathy, J. C. Sehra, and A. V. Kulkarni, J. Mater. Chem. **11**, 691 (2001).
[8] Z. Yang, P. Cai, L. Chen, Y. Gu, L. Shi, A. Zhao, and Y. Qian, J. Alloys Compd. **420**, 229 (2006).
[9] C. L. Yeh, H. C. Chuang, E. W. Liu, and Y. C. Chang, Ceram. Int. **31**, 95 (2005).
[10] H. Subramanya Herle, M. S. Hegde, N. Y. Vasathacharya, and S. Philip, J. Solid State Chem. **134**, 120 (1997).
[11] I. Galesic and B. O. Kolbesen, Fresenius' J. Anal. Chem. **365**, 199 (1999).
[12] J. M. Cordoba, M. J. Sayagues, M. D. Alcala, and F. J. Gotor, J. Am. Ceram. Soc. **90**, 381 (2007).
[13] P. Ferrer, J. E. Iglesias, and A. Castro, Chem. Mater. **16**, 1323 (2004).
[14] J. M. Xue, D. M. Wan, and J. Wang, Mater. Lett. **39**, 364 (1999).
[15] C. Suryanarayana, Prog. Mater. Sci. **46**, 1 (2001).
[16] F. J. Gotor, M. D. Alcala, C. Real, and J. M. Criado, J. Mater. Res. **17**, 1655 (2002).
[17] J. M. Criado, M. D. Alcalá, and C. Real, Solid State Ionics **101–103**, 1387 (1997).
[18] D. Wexler, A. Calka, and A. Y. Mosbah, J. Alloys Compd. **309**, 201 (2000).
[19] A. Calka and J. S. Williams, Mater. Sci. Forum **88–90**, 787 (1992).
[20] B. K. Teo, *EXAFS: Basic Principles and Data Analysis* (Springer-Verlag, New York, 1986); D. C. Koningsberger and R. Pins, *X-Ray Absorption: Principles, Applications, Techniques of EXAFS, SEXAFS, and XANES* (Wiley, New York, 1988).
[21] F. J. Gotor, M. D. Alcalá, C. Real, and J. M. Criado, J. Mater. Res. **17**, 1655 (2002).
[22] G. R. Castro, J. Synchrotron Radiat. **5**, 657 (1998).
[23] C. Dong and J. I. Langford, J. Appl. Crystallogr. **33**, 1177 (2000).
[24] F. Carrera, E. Sanchez Marcos, P. J. Merkling, J. Chaboy, and A. Muñoz-Páez, Inorg. Chem. **43**, 6674 (2004).
[25] J. W. Cook and D. E. Sayers, J. Appl. Phys. **52**, 5024 (1981).
[26] M. Newville, J. Synchrotron Radiat. **8**, 322 (2001); E. A. Stern, M. Newville, B. Ravel, Y. Yacoby, and D. Haskel, Physica B (Amsterdam) **208–209**, 117 (1995).
[27] J. Mustre de Leon, J. J. Rehr, S. I. Zabinsky, and R. C. Albers, Phys. Rev. B **44**, 4146 (1991); S. I. Zabinsky, J. J. Rehr, A. Ankudinov, R. C. Albers, and M. J. Eller, *ibid.* **52**, 2995 (1995); A. L. Ankudinov, B. Ravel, J. J. Rehr, and S. D. Conradson, *ibid.* **58**, 7565 (1998).
[28] S. Diaz-Moreno, A. Muñoz-Páez, and E. Sanchez Marcos, J. Phys. Chem. B **104**, 11794 (2000).
[29] T. Yokoyama, K. Kobayashi, T. Ohta, and A. Ugawa, Phys. Rev. B **53**, 6111 (1996).
[30] P. J. Merkling, A. Muñoz-Páez, and E. Sanchez Marcos, J. Am. Chem. Soc. **124**, 10911 (2002).
[31] J. J. Rehr, R. C. Albers, and S. I. Zabinsky, Phys. Rev. Lett. **69**, 3397 (1992); P. A. O'Day, J. J. Rehr, S. I. Zabinsky, and G. E. Brown, Jr., J. Am. Chem. Soc. **116**, 2938 (1994).
[32] C. L. Yeh, H. C. Chiang, E. W. Liu, and Y. C. Chang, Ceram. Int. **31**, 95 (2005).
[33] H. Kwon, S. Chot, and L. T. Thompson, J. Catal. **184**, 236 (1999).
[34] P. Malet, A. Muñoz-Páez, C. Martín, and V. Rives, J. Catal. **134**, 47 (1992).
[35] J. Wong, F. W. Lytle, R. P. Messmer, and D. H. Maylotte, Phys. Rev. B **30**, 5596 (1984).
[36] P. P. Chatterjee, S. K. Pabi, and I. Manna, J. Appl. Phys. **86**, 5912 (1999).
[37] I. Manna, P. P. Chattopadhyay, P. Nandi, F. Banhart, and H. J. Fecht, J. Appl. Phys. **93**, 1520 (2003).
[38] I. Manna, P. P. Chattopadhyay, F. Banhart, and H. J. Fecht, Appl. Phys. Lett. **81**, 4136 (2002).
[39] M. D. Alba, R. Alvero, A. I. Becerro, M. A. Castro, A. Muñoz-Páez, and J. M. Trillo, J. Phys. Chem. **100**, 19559 (1996).
[40] L. M. Colyer, G. N. Greaves, A. J. Dent, K. K. Fox, S. W. Karr, and R. H. Jones, Nucl. Instrum. Methods Phys. Res. B **97**, 107 (1995).
[41] R. B. Greegor and F. W. Lytle, J. Catal. **63**, 476 (1980).
[42] S. Diaz Moreno, D. C. Koningsberger, and A. Muñoz-Páez, Nucl. Instrum. Methods Phys. Res. B **133**, 15 1997.
[43] A. Muñoz-Páez, J. I. F. Peruchena, J. P. Espinós, A. Justo, F. Castañeda, S. Díaz-Moreno, and D. T. Bowron, Chem. Mater. **14**, 3220 (2002).
[44] E. A. Stern, Phys. Rev. B **48**, 9825 (1993).
[45] J. W. Christian, *The Theory of Transformation in Metals and Alloys* (Pergamon, Oxford, 1978).